# Photoemission electron microscopy using extreme ultraviolet attosecond pulse trains

Mikkelsen, Anders; Schwenke, Jörg; Fordell, Thomas; Luo, Gang; Klünder, Kathrin; Hilner, Emelie; Anttu, Nicklas; Zakharov, Alexei; Lundgren, Edvin; Mauritsson, Johan; Andersen, Jesper N; Xu, Hongqi; L'Huillier, Anne

Link to publication

# Photoemission electron microscopy using extreme ultraviolet attosecond pulse trains

A. Mikkelsen,[1] J. Schwenke,[1] T. Fordell,[1] G. Luo,[1] K. Klünder,[1] E. Hilner,[1] N. Anttu,[1] A. A. Zakharov,[2] E. Lundgren,[1] J. Mauritsson,[1] J. N. Andersen,[1] H. Q. Xu,[1] and A. L'Huillier[1]

[1]*Department of Physics, Lund University, Box 118, 22100 Lund, Sweden*
[2]*MAX-lab, Lund University, Box 118, 22100 Lund, Sweden*

We report the first experiments carried out on a new imaging setup, which combines the high spatial resolution of a photoemission electron microscope (PEEM) with the temporal resolution of extreme ultraviolet (XUV) attosecond pulse trains. The very short pulses were provided by high-harmonic generation and used to illuminate lithographic structures and Au nanoparticles, which, in turn, were imaged with a PEEM resolving features below 300 nm. We argue that the spatial resolution is limited by the lack of electron energy filtering in this particular demonstration experiment. Problems with extensive space charge effects, which can occur due to the low probe pulse repetition rate and extremely short duration, are solved by reducing peak intensity while maintaining a sufficient average intensity to allow imaging. Finally, a powerful femtosecond infrared (IR) beam was combined with the XUV beam in a pump-probe setup where delays could be varied from subfemtoseconds to picoseconds. The IR pump beam could induce multiphoton electron emission in resonant features on the surface. The interaction between the electrons emitted by the pump and probe pulses could be observed. © *2009 American Institute of Physics.* [doi:10.1063/1.3263759]

## I. INTRODUCTION

A photoemission electron microscope (PEEM) images surfaces using photoelectrons generated by a light source with photon energies exceeding the work function threshold (usually 4–5 eV). The photoelectrons are accelerated in an electric field, focused, and imaged with a resolution down to the nanometer scale.[1,2] The versatility of PEEM as a tool to study ultrafast processes with high lateral resolution has been demonstrated in a number of cases.[3–12] This ranges from ultrafast magnetic processes in micro- and nanostructures occurring in the picosecond range to electron excitation such as plasmons and transient states in nanostructures occurring in the femtosecond range. Two types of pump-probe measurements were typically performed: first, the time structure of electron bunches in synchrotron rings provided short probe pulses, which were correlated with either laser or electrical pump pulses. Second, frequency doubled infrared (IR) femtosecond lasers have been used, requiring two-photon processes to exceed the work function threshold. The latter type of experiment is especially suited to study electric field enhancement as the photoemission yield will scale as the field strength to the power of 4, resulting in high sensitivity to variations in the electric field.

State-of-the-art laser systems are nowadays capable of producing ultrashort extreme ultraviolet (XUV) pulses well in the attosecond regime,[13,14] which in combination with a PEEM should allow for extreme temporal and high spatial resolution simultaneously when probing collective electron excitation and motion. Recently, it was suggested by Stockman *et al.*[15,16] to use synchronized ultrashort IR and XUV light pulses to study plasmon dynamics in a pump-probe

scheme. Such a setup, which we abbreviate "atto-PEEM," is limited in time resolution only by the pulse duration of the XUV probe field, in the 100 as range. Stockman *et al.*[15,16] further suggested that by using a time-of-flight (TOF) detector in the PEEM to gain energy resolution, the microscope can directly probe the nanoplasmonic field strength with nanometer resolution. The idea is that the IR pump pulse creates nanoplasmonic fields at various sites on the surface. As the photoelectrons excited by the XUV probe pulse then leave the surface, their escape speed will be changed by the presence of the nanoplasmonic field. This will manifest itself in a significant increase or decrease in the electron energies as measured in the TOF system, which can then be related to the strength of the nanoplasmonic fields.

We propose, as opposed to directly probe the electrical fields, to measure the lateral changes in electron density on the surface induced by the nanoplasmonic fields. This should be visible as a change in the number of photoelectrons released by the XUV pulse at specific positions. Measurements of the spatial electron density can, in principle, be carried out with less stringent demands on energy filtering capabilities, while still revealing important information on plasmon dynamics. Surface charges will oscillate back and forth across nanoplasmonic features such as holes or particles during a cycle of the electric field.[17–19] The electron density should appear asymmetric as the extremes of the electric field cycle are reached.[17–19]

Conceptually, the most straightforward IR/XUV experiment involves a single femtosecond IR pump pulse, followed by a single attosecond XUV probe pulse. By varying the time delay between the IR electric field and the attosecond
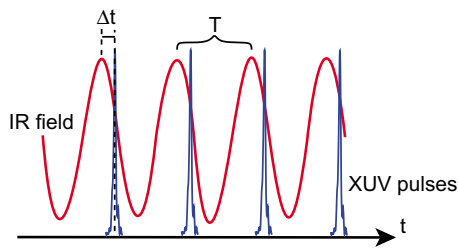
FIG. 1. (Color online) Schematic of the oscillating field of the IR laser beam and the XUV pulse train. It is possible to align the distance between the XUV attosecond pulses with the cycle period T of the electric field. The delay between the train and the IR field can now be varied with high precision. Charge oscillations on the surface following the IR pulse (such as surface plasmons) should now be visible by comparing images obtained at different delays (Δt).
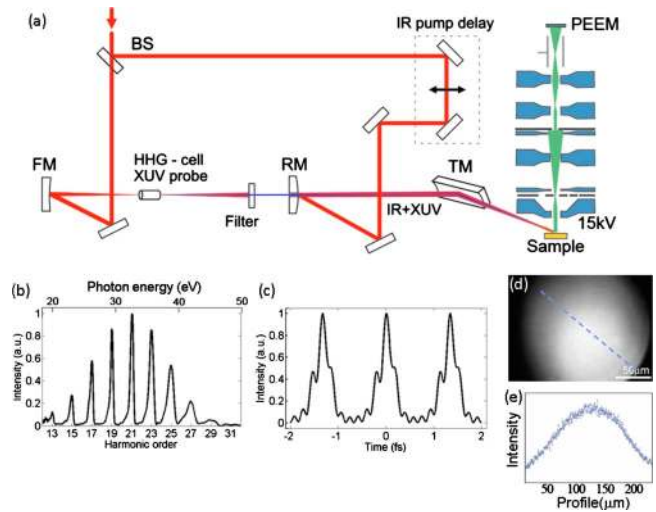


FIG. 2. (Color online) (a) Schematic model of the experimental setup. The label BS denotes the beam splitter, FM the focusing mirror, RM the recombination mirror, and TM the toroidal mirror. (b) Energy structure of the XUV beam recorded with a magnetic-bottle TOF spectrometer. (c) Time structure of the XUV attosecond pulses in the central part of the train with a 200 nm Al filter. (d) 3 kV low magnification PEEM image of the electron emission spot from the XUV laser pulse at high intensity. (e) Profile measured across (d), as indicated by the broken (blue) line in (d).

pulse, the time evolution of a single surface plasmon excitation can be investigated on an attosecond time scale. Another interesting possibility is to use a single femtosecond IR pump pulse and a synchronized attosecond pulse train, with, for example, one pulse per IR cycle.[20] This type of experiment is displayed in Fig. 1, indicating how the different delays between the pulse train and the IR field oscillation can be used to probe the cycle of the charge excitations on the surface. Such an experiment could be advantageous for observation of plasmons on a surface since the number of useful probe pulses increases, but it would make it more difficult to measure the delay of a plasmonic excitation over a relatively long (femtosecond) time scales.

In this paper, we demonstrate imaging with trains of attosecond pulses (width of 200 as, energy spread of 10–30 eV) using a Focus IS-PEEM with no special energy filtering. We resolve structures having widths down to 200–300 nm and show that at present our spatial resolution is limited by the lack of energy filtering used in the PEEM experiment, a problem that can be solved using either a more advanced version of the PEEM or by introducing small contrast apertures. The time resolution is, in principle, given by the pulse width of the attosecond pulses, but this could not be directly verified.

## II. EXPERIMENT

A schematic drawing of the experimental setup is shown in Fig. 2(a). A chirped pulse amplifier system operating at 800 nm delivers pulses of 35 fs length and energy of 3.6 mJ at a repetition rate of 1 kHz. A fraction of the pulse energy is split off to a delay stage and used as a pump beam, while the major part is focused with a f=75 cm mirror into a 6 mm long pulsed argon gas jet for high-harmonic generation (HHG). The emerging XUV emission from the gas cell is subsequently spatially and spectrally filtered using a small aperture and metallic filters to provide trains of about 10 pulses with 200 as pulse duration and a separation of 1.3 fs. Figure 2(b) shows a typical spectrum of the generated XUV beam, and Fig. 2(c) shows the time structure of the attosecond pulse train. The number of photons is estimated to be $10^7-10^8$ photons per shot per harmonic. As discussed in more detail below, this result in the release of $\sim 10^7$ photoelectrons from a gold surface in each pulse, and thus only a

fraction of the total flux can be used in the PEEM experiment due to space charge effects. The metallic filters used include 200 nm Al, 400 nm Al, and 200 nm Al+200 nm Sn. The energy range is 18–55 eV with the Al filter, which can be further reduced to a narrow bandwidth around 20 eV by additionally applying a Sn filter. The filtered XUV beam is combined with the IR pump beam with a recombination mirror and finally focused onto the sample stage of the PEEM with a toroidal mirror (focal length of 30 cm).

The PEEM is a commercial Focus IS-PEEM supplied by Omicron,[21] as schematically shown in Fig. 2(a). Photoelectrons are extracted from the sample stage with voltages of up to 15 kV and focused using an electrostatic focusing system. The test setup used in these measurements relies on a turbopump for vacuum, with no special damping, and the PEEM had no highpass/bandpass energy filter. Nevertheless, resolution down to 100 nm could be achieved with a standard mercury arc light source, as discussed below. The PEEM vacuum chamber is directly connected to the HHG vacuum chamber. Alignment of the PEEM could be done via XY boards on the vacuum system base and guided by the IR laser beam used to generate the XUV radiation and usually cut by Al filters, which is therefore superimposed on the XUV beam. Final alignment and initial characterization of the XUV beam is done using the PEEM in low magnification (3 kV), as shown in Figs. 2(d) and 2(e).

The setup was first tested with a lithographic sample, described here: the sample consisted of a Si substrate with a 65 nm thick patterned Au film. Figure 3(a) shows a scanning electron microscopy (SEM) image of one of the fabricated structures used in this work. Figure 3(b) shows a schematic of the negative resist structure. The patterned film was made using electron beam lithography (EBL) as follows. First, a negative EBL resist ma-N 2403 was spin coated on the wafer at 3000 rpm and baked at 90 °C for 60 s. The thickness of
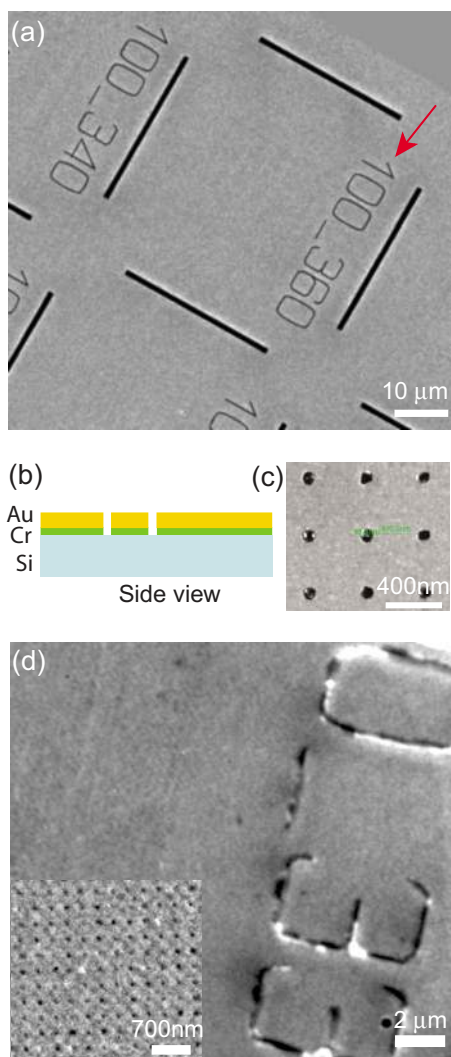
FIG. 3. (Color online) (a) SEM image of part of the lithographic pattern. In total, nine square arrays of holes were fabricated in a square region of $150 \times 150$ $\mu m^2$ of the Au film. [The magnification in this image is so low that the hole arrays cannot be seen, instead see Fig. 3(c).] Each region is divided using 1 $\mu m$ wide lithographic lines, and at the center of each divided region there is an array of holes covering a $20 \times 20$ $\mu m^2$ area. The hole diameter and the separation is indicated using text numbers fabricated lithographically with 200 nm wide text lines—the arrow points to this text line. (b) Schematic of the lithographic sample. The Au film is connected to the sample holder to minimize charging effects. (c) SEM image of a small part of the hole array with 100 nm in hole diameter and 400 nm in hole separation. (d) PEEM image recorded with an extractor voltage of 14 kV using a standard Hg lamp ($h\nu < 4.9$ eV) for illumination. The image shows part of a structure similar to the one in Fig. 2(a). The inset shows the array of 100 nm holes as imaged by PEEM indicating that the PEEM can obtain a resolution of $<50$ nm. The holes could only be clearly seen when the PEEM was run with an ion pump and no turbopumps on.

the resist was about 300 nm. The electron beam exposure was performed on a Raith 150 e-beam writer with an exposure dose of 300 $\mu C/cm^2$. After exposure, the resist was developed with ma-D532 for 30 s and then rinsed with water for 10 min. Finally, 5 nm thick Cr and 65 nm thick Au were evaporated on the wafer and lift-off was performed in Remover 1165. Nine arrays of holes were made in a 150 $\times 150$ $\mu m^2$ region of the Au film. The region was divided into nine $50 \times 50$ $\mu m^2$ squares using 1 $\mu m$ wide lines. At the center part of each square, there is an array of holes with



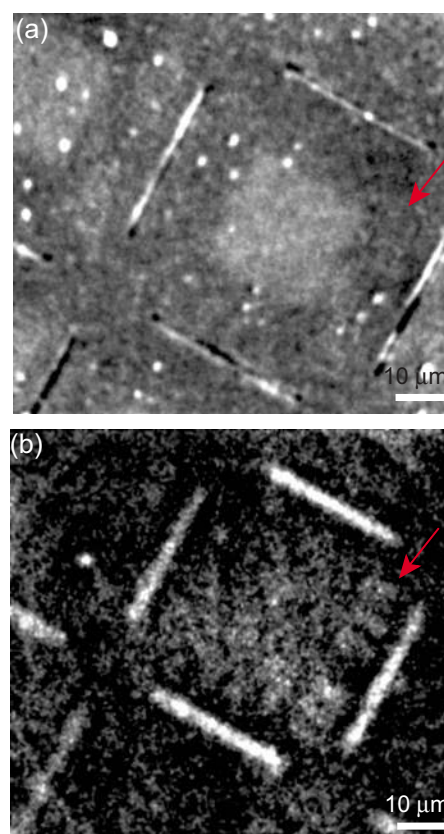FIG. 4. (Color online) (a) PEEM image recorded with an extractor voltage of 14 kV using a standard Hg lamp ($h\nu < 4.9$ eV) for illumination. The image shows the same structure similar to the one in Fig. 2(a). (b) PEEM image recorded under the same conditions using XUV attosecond pulse trains with a max energy of 30 eV. Notice that in both cases the 1 $\mu m$ broad lines can be clearly observed, while also the text can be observed as indicated by the arrows. The structure obtained with the XUV beam is not as sharp as with the Hg lamp and we estimate that our resolution has dropped to $\sim 200$ nm.

a coverage area of $20 \times 20$ $\mu m^2$. The diameter of the holes was 100 nm in all the nine arrays and the separation between holes was designed to be different in different arrays and was systematically changed from 240 to 400 nm. The hole diameter and the separation between holes in each hole array were indicated by text numbers made lithographically with 200 nm wide text lines.

Other structures imaged in this test experiment were size-selected 50 nm Au aerosol nanoparticles, deposited on a conducting Si substrate with a density of $1/\mu m^2$, as well as 35 nm III-V nanowires which were also deposited on a conducting Si substrate. Growth and deposition of these structures were described previously.[22,23]

## III. RESULTS AND DISCUSSION

From Fig. 3, it can be concluded that the PEEM used with a Hg lamp has a resolution of $<50$ nm. To study the extent to which resolution in the present setup was limited by mechanical vibrations introduced by a running turbopump, we imaged the lithographic structure again using a standard Hg lamp [Fig. 4(a)]. From these images, we estimate that we

can still resolve features down to at least ∼100 nm despite having made no serious efforts to mechanically damp the system.

Figure 4(b) shows the lithographic structure imaged with the XUV attosecond pulse train. To obtain a sharp image, we had to turn down the gas pressure in the HHG cell. The pressure measured in the chamber was reduced from 3.2 to 0.06 $\mu$bar or below. The harmonic yield varies as the square of the pressure at lower pressures, but gets saturated at a higher pressure. We estimate the reduction in the signal to at least a factor of 100. Also, a 200 nm Al filter was added, reducing the light intensity by an additional factor of 3, depending on the degree of oxidation of the filters. Altogether, we estimate the necessary reduction in the XUV intensity to more than a factor 300. At higher XUV intensity, the images gradually became blurred until only the broad (>200 $\mu$m in diameter) footprint of XUV beam was observed. The intensity of the XUV beam could still be reduced a factor of 10 below the threshold (where no blurring occurred) without observing any further changes in the image except for the expected reduction in intensity. The blurring can be understood in terms of space charge effects: although the average electron density on the scale of seconds (as is the exposure time of the PEEM) is relatively moderate, the short duration of the XUV pulses leads to high peak photon intensities, in the range $10^8 – 10^9$ W/cm$^2$. Put in another way, with a total length of each pulse train of ∼20 fs and a repetition rate of 1 kHz, the intensity of each pulse will be $10^{12}$ higher than the intensity of the field from a cw XUV source with the same average power. As a result, the average electron density generated by each pulse will also be very high. This will lead to Coulomb repulsion, which can manifest itself in three ways: temporal broadening, longitudinal broadening, and energy broadening. The longitudinal broadening and energy broadening can both lead to significant blurring of the images, while the energy broadening in this case is probably less relevant as we already have a very broad energy spectrum.

As in previous work,[24] the number of photoelectrons emitted per pulse can be quantitatively estimated for our gold films using the photoionization cross section, atom density, and electron mean free path of gold for photons with an energy around 30 eV.[25,26] Thus, we can estimate the photoelectron emission to ∼$10^7$ electrons per pulse train at the maximum power of the laser system. As the spot size is roughly 250 $\mu$m in diameter and we have 1000 pulse trains per second, this corresponds to ∼200 000 $e$/s $\mu$m$^2$. This can be compared to the measured sample current generated by the Hg lamp, which taking the larger footprint of the Hg lamp spot into account gives ∼8000 $e$/s $\mu$m$^2$. This agrees with our observation that the maximum intensity achievable using the laser system is much higher than the intensity from the Hg lamp. However, we also find that we can reduce the peak intensity of the laser system to avoid space charge problems, while still generating enough photoelectrons on average to form an image. In this situation, we compare images from similar structures made using the standard Hg lamp or the attenuated XUV laser. We find that we now have to increase exposure times by a factor of 2–4 for the XUV imaging to achieve the same image intensities as with the Hg
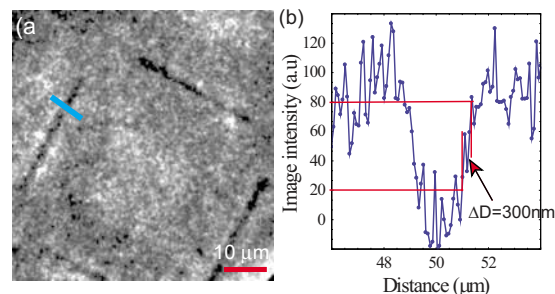


FIG. 5. (Color online) (a) PEEM image of the lithographic structure using the XUV laser source at a different focus, where the central square containing the hole array can be seen and the marking lines appear black. (b) Profile averaged along the 1 $\mu$m wide lithographic. The distance 20% from the bottom to 80% from the top of the troughs can be used as a different measure of resolution with a result of ∼300 nm.

lamp. This is in reasonable agreement with the estimates made above and it is important to note that we could still reduce the intensity of the laser by another factor of 5–10 before completely losing the possibility to perform imaging.

In our experiment and from the calculations above we can deduce that the threshold electron density for avoiding space charge problems is ∼2 $e/\mu$m$^2$ pulse. Theoretical and experimental works on short electron pulses[27–29] and photoemission[30,31] have shown that similar space charge problems also appear at a threshold around 2 $e/\mu$m$^2$ pulse,[27] in good agreement with our results. Generally, it was found that while longitudinal broadening of electron pulses can be very significant at the values found also in our case, energy broadening would typically be up to a few eV. As we already have an energy distribution of ∼30 eV, we believe that the energy broadening will not cause much additional geometric smearing of the image.

Our results can also be compared to results obtained using the femtosecond XUV pulses from the free-electron laser at Hamburg.[24] For photoemission energy spectra, space charge effects were observed at a threshold of ∼$10^5$ electrons/pulse, with a similar footprint as our laser beam, which is in good agreement with the threshold for space charge effects found for the attosecond pulses in our experiment. Interestingly, it was recently found that in the two-photon or three-photon photoemission microscopy experiments using a laser system operating at 1 kHz repetition rate (as ours) intensity had to be reduced to levels where imaging was only possible by measurements over 15 min.[32] In this case the space charge problems are believed to occur at the hemispherical energy analyzer incorporated in the design, a feature not installed in our PEEM. Thus, it seems quite conceivable that the specific design of the PEEM will very much influence the degree of space charge problems observed, especially if electrons are decelerated in the PEEM as is the case in the hemispherical analyzer described in Ref. 32.

In the image seen in Fig. 4(b), the thick lines and even the lithographic text (to some extent) can be seen. As the text lines are 200 nm wide, this indicates that objects down to a size of 200 nm can be discerned. Further, we find, as seen in Fig. 5(a), that changing the focus of the PEEM leads to the possibility of observing the dot arrays at the center, though still no features below 200 nm are seen. Finally, we have
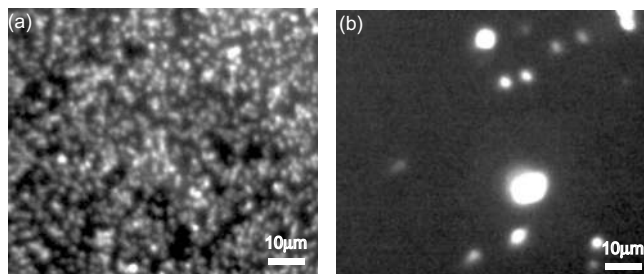
FIG. 6. (Color online) (a) PEEM image (extraction voltage of 14 kV) of Au aerosol nanoparticles of 50 nm in diameter recorded with the standard Hg lamp as photon source. (b) PEEM image (extraction voltage of 14 kV) of the same area with Au aerosol nanoparticles of 50 nm in diameter as in Fig. 4(b), recorded with a 35 fs IR pulse with a photon energy of 1.55 eV. Some points can be observed presumably corresponding to two or more Au particles with interparticle distances leading to plasmon resonances for this IR wavelength (Ref. 36), thus allowing considerable multiphoton electron emission.



FIG. 7. (Color online) (a) $40 \times 40$ $\mu$m$^2$ PEEM image of nanowires dispersed on a Si surface recorded using monochromatized 34 eV photons from the MAX-II synchrotron with an Elmitec SPELEEM system. An energy filter of 0.7 eV was used. One nanowire is indicated by the light gray (blue) arrow, while two larger features are indicated by the dark gray (red) arrow. (b) $40 \times 40$ $\mu$m$^2$ PEEM image of the same area as in (a). The energy filter was removed and only the background structure of the PEEM micro channel plate and a few large features can be observed [at the (red) arrow]. (c) $40 \times 40$ $\mu$m$^2$ PEEM image of the same area as in (a). A small contrast aperture was inserted and again small features can be observed.

measured the profile across the 1 $\mu$m wide lines in the pattern and find that using a span of 20%–80%, as seen in Fig. 5(b), the resolution is less than 300 nm. We therefore estimate the spatial resolution limit of the atto-PEEM system to be between 200 and 300 nm at present.

To further explore the experimental setup, we also imaged a sample with Au aerosol nanoparticles with a diameter of 50 nm. The image obtained with the Hg lamp is seen in Fig. 6(a), while an image obtained with the 35 fs IR pump pulse (photon energy of 1.55 eV) is seen in Fig. 6(b). The 50 nm Au particles can be clearly seen with the Hg lamp, and some multiphoton excitation is observed with the IR laser (as discussed more below). However, we did not observe the particles using XUV light. From changing the XUV light intensity, we see no indication that this effect is due to space charge effects. We believe that the limitation in resolution is mainly due to the energy spread of the photoelectrons—chromatic aberration. This is not a problem for the multiphoton emission induced by the IR beam, which will result in electrons within a narrow energy range just above the work function threshold. Because the XUV light has photon energies from 15 to 40 eV, the emitted photoelectrons will have an energy spread from 0 to 35 eV, when taking into account the ~5 eV work function of the material. As our PEEM does not have an electron energy filter, we see electrons with all kinetic energies in the image. This results in a certain blurring due to the different paths taken by electrons of different energies originating from the sample position. The problem of chromatic aberration in PEEM is well known.[33] Crude low-pass electron energy filtering can be achieved by using small enough contrast apertures (as also found in our PEEM), however, at the cost of significant loss of intensity. As the charge coupled device camera presently used in our PEEM is not suitable for long exposures/low intensities, we could only use the two largest apertures, with no energy filtering effect.[34]

To check if this chromatic aberration could explain our spatial resolution limit using photon energies around 30 eV, we made a test at the Elmitec SPELEEM system situated at the MAX-II synchrotron ring at MAX-laboratory.[35] Using 34 eV photons from a synchrotron beamline we imaged semi-
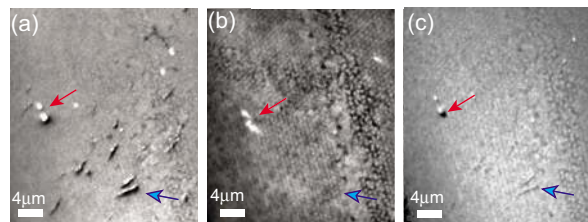
conductor nanowires, with diameters of 35 nm and length of several microns, spread randomly across a Si substrate. The image recorded with an energy bandpass filter (0.7 eV) can be seen in Fig. 7(a). Nanowires randomly spread on the substrate are observed. Removing the energy filter (resulting in a bandwidth of >10 eV), and imaging the same area, as seen in Fig. 7(b), we find that virtually all nanowires in the image have disappeared and only large features wider than 100 nm wide can be seen. Our experiment demonstrate that imaging using ~30 eV photons without an energy filter results in resolution being limited to >100 nm. This suggests that a normal spatial resolution of 50 nm or below could be achieved with the atto-PEEM by introducing an energy filter in the PEEM. This will result in a loss of photoelectron intensity, which can be compensated by extending the exposure time in order to obtain images of reasonable quality. A small contrast aperture may also act as a low-pass energy filter. We demonstrate this in Fig. 7(c) where we have inserted a small contrast aperture and smaller features again appear at the center of the image, albeit with significant loss of intensity.

Finally, we have tested a full experimental pump-probe setup including 35 fs 800 nm IR pulses and XUV attosecond pulse trains: atto-PEEM. The pulses were spatially superposed in space and the time delay between them could be controlled from the subfemtosecond level up to a few picoseconds.[17] In Figs. 8(a)–8(c) we show images of the lithographic structures illuminated with XUV, IR, and XUV+IR, respectively. The IR beam is powerful enough to induce photoelectron emission from the sample even when strongly attenuated. Emission occurs primarily from points within the broad lines in the lithographic structure. Two-photon plasmon resonance enhancement has been imaged in PEEM previously;[12] however, since the photon energy is only 1.55 eV, multiphoton processes are needed to excite electrons above the work function threshold (4–5 eV for Si and Au). In addition, resonant enhancement must presumably occur, which increases the field locally and thus the number of multiphoton processes. Geometric features that enhance the fields of the IR laser beam would have a rather specific size and shape.[12,19,35] Electron emission due to multiphoton and thermionic electron emission have been observed for IR
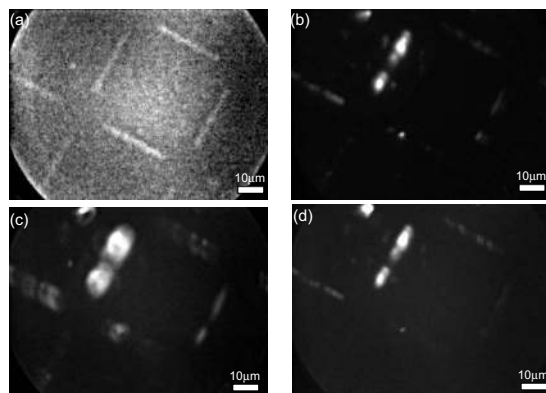
FIG. 8. (a) PEEM image (12 kV) of lithographic structure recorded using the XUV beam. (b) PEEM image (12 kV) of the same structure and area using the 1.55 eV IR laser beam. (c) PEEM image (12 kV) of the same structure and area using the 1.55 eV IR laser beam and the XUV beam with no time delay between the two beams. (d) PEEM image (12 kV) of the same structure and area using the 1.55 eV IR laser beam and the XUV beam with a time delay of 10 ps between the two beams.

lasers systems[36] in the presence of Au and Ag nanoparticles. Photoelectrons are only excited from a few points on the surface, indicating that indeed very special morphological conditions have to be present.

Returning for a moment to the Au nanoparticles, imaged in Fig. 6, we find that emission induced by the IR beam only occur in a few points which again would indicate that resonant enhancement occurs at a few Au particle pairs separated by a distance matched to the laser wavelength or overlapping in specific configurations.[36] Combining the XUV and IR beam, as seen in Fig. 8(c), it can be observed that the IR and XUV beams influence each other, seen as a defocusing of the image. We have investigated this influence as a function of delay between the IR and the XUV beam and we find that the effect clearly diminishes on a picosecond time scale. The effect is observed both when the XUV pulse is before and after the IR pulse. This would indicate an effect where the electric fields from the charges created by the two pulses influence each other. Such effects should be most important at the point where the charges are closest to each other and therefore most concentrated. Charge density is generally highest in the focal points of the PEEM—thus, the back focal plane or the area near the sample would be a candidate. The distance between the two charge pulses will be smallest in the region between the extractor and the sample where they are accelerated up. In a simple model,[27] the central position of a electron pulse in this region will vary as $z(t) = (eV_0 t^2)/(2md)$, where z is the distance between the pulse and the sample, d is the distance between the extractor and the sample, m is the electron mass, $V_0$ is the extractor voltage (set to 14 kV), and e is the electron charge. From this formula we calculate that the total time spent in the extractor region is 60 ps. Assuming that the two pulses generated are separated by 5 ps, we calculate that after the second pulse is released, the distance between the two pulses is between 15 and 80 $\mu$m during the first 10 ps—less than the estimated diameter of the pulses of ~250 $\mu$m. The separation between the pulses after they leave the accelerating field can be calculated to be ~350 $\mu$m. This is also the distance between
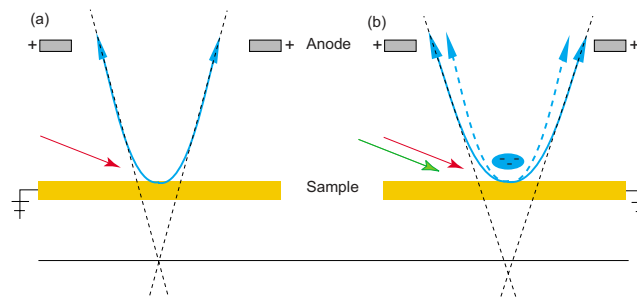


FIG. 9. (Color online) Simplified illustration of the mechanism behind the interaction of the electrons created by the IR and the XUV pulses, respectively (Refs. 37 and 38). The first stage of the PEEM lens system consists of the sample as cathode and the first lens of the PEEM as anode. (a) If only one electron excitation source (indicated by the arrows) is used, the electron paths [indicated by solid (blue) lines] will pass into the microscope being bend by the first lens, thus effectively creating a focus point behind the sample (Refs. 37 and 38). The focus point of the PEEM behind the sample is indicated by the crossing of the broken black lines. (b) If two consecutive excitation pulses follows rapidly after each other (indicated by the arrows). The electric field from the charges excited from the first pulse will act to bend the trajectories of the electrons excited by the second pulse. This also effectively moves the focus point. For some special cases it will be possible to move the focus point back by then changing the focus of the PEEM.

the two pulses in the back focal plane. Thus, we estimate that the interaction between two pulses, when separated in time, is strongest near the sample. In a simple model of the first stage of the PEEM and the sample described as a cathode/anode lens,[37,38] the observed effect can be understood as a result of the field from the photoelectrons released by the XUV pulse effectively spreading out the photoelectrons from the IR pulse, as indicated in Figs. 9(a) and 9(b)—thus, acting as an additional electrostatic element in the system. As is also observed, this effect would exist no matter which pulse comes first as the photoelectron bunches would affect each other while moving through the lens system of the PEEM. Finally, if the charge created by one pulse acts as a simple electrostatic lens on the other pulse moving the focal point (as also shown in Fig. 9), one can, under some conditions, refocus the spots in the images by changing the focus of the PEEM. Indeed, we find that by changing the focus of the PEEM we can refocus the bright spots of electrons emitted due to the IR beam. Finally, we have observed that this space charge effect can also be removed be reducing the intensity of the IR beam, while still observing multiphoton electron emission.

## IV. CONCLUSIONS

In this work, we demonstrated that the attosecond pulse trains generated by a kilohertz laser system provide sufficient average photon flux for PEEM experiments. We noticed that the spatial resolution of the measurements is limited by the energy spread in the photoelectron beam. This problem can be resolved by filtering the electron beam in the imaging column of the PEEM either using small contrast apertures or other energy filtering schemes.

We find that the pump IR beam in the experimental system is strong enough to induce strong multiphoton electron emission at resonant nanoscale features on the surface. The photoelectrons emitted from the pump and probe beams are

found to affect each other through the lens system. We have observed that by turning down the intensities of the pump and probe beams the effects diminish.

The peak intensity of the attosecond probe beam needs to be attenuated to avoid space charge effects. To increase the average photon flux, thus allowing us to obtain higher quality images by energy filtering, one would need a repetition rate higher than the 1 kHz of the present system. High power laser systems, with repetition rates between 100 kHz and 1 MHz, are under development.[39,40] An elegant solution to this problem may also be to generate the high-order harmonic beam by plasmon resonance field enhancement in nanoscale arrays.[41] Such a system could operate with a megahertz repetition frequency, thus increasing the average intensity while individual peak intensities could be kept low.

## ACKNOWLEDGMENTS

[1] E. Bauer, J. Phys.: Condens. Matter **13**, 11391 (2001).

[2] A. Locatelli, L. Aballe, T. O. Mentes, M. Kiskinova, and E. Bauer, Surf. Interface Anal. **38**, 1554 (2006).

[3] G. Schönhense and H. J. Elmers, Surf. Interface Anal. **38**, 1578 (2006).

[4] A. Krasyuk, A. Oelsner, S. A. Nepijko, A. Kuksov, C. M. Schneider, and G. Schonhense, Appl. Phys. A: Mater. Sci. Process. **76**, 863 (2003).

[5] J. Raabe, C. Quitmann, C. H. Back, F. Nolting, S. Johnson, and C. Buehler, Phys. Rev. Lett. **94**, 217204 (2005).

[6] J. Vogel, W. Kuch, M. Bonfim, J. Camarero, Y. Pennec, F. Offi, K. Fukumoto, J. Kirschner, A. Fontaine, and S. Pizzini, Appl. Phys. Lett. **82**, 2299 (2003).

[7] C. M. Schneider, A. Kuksov, A. Krasyuk, A. Oelsner, and D. Neeb, Appl. Phys. Lett. **85**, 2562 (2004).

[8] S. B. Choe, Y. Acremann, A. Scholl, A. Bauer, A. Doran, J. Stohr, and H. A. Padmore, Science **304**, 420 (2004).

[9] A. Krasyuk, F. Wegelin, S. A. Nepijko, H. J. Elmers, G. Schönhense, M. Bolte, and C. M. Schneider, Phys. Rev. Lett. **95**, 207201 (2005).

[10] O. Schmidt, M. Bauer, C. Wiemann, R. Porath, M. Scharte, O. Andreyev, G. Schönhense, and M. Aeschlimann, Appl. Phys. B: Lasers Opt. **74**, 223 (2002).

[11] M. Cinchetti, A. Gloskovskii, S. A. Nepjiko, G. Schönhense, H. Rochholz, and M. Kreiter, Phys. Rev. Lett. **95**, 047601 (2005).

[12] A. Kubo, K. Onda, H. Petek, Z. Sun, Y. S. Jung, and H. K. Kim, Nano Lett. **5**, 1123 (2005).

[13] R. López-Martens, K. Varjú, P. Johnsson, J. Mauritsson, Y. Mairesse, P. Salières, M. B. Gaarde, K. J. Schafer, A. Persson, S. Svanberg, C.-G. Wahlström, and A. L'Huillier, Phys. Rev. Lett. **94**, 033001 (2005).

[14] R. Kienberger, Science **297**, 1144 (2002).

[15] M. I. Stockman, M. F. Kling, U. Kleineberg, and F. Krausz, Nat. Photonics **1**, 539 (2007).

[16] J. Lin, N. Weber, A. Wirth, S. H. Chew, M. Escher, M. Merkel, M. F. Matthias, M. I. Stockman, F. Krausz, and U. Kleineberg, J. Phys.: Condens. Matter **21**, 314005 (2009).

[17] S. K. Ghosh and T. Pai, Chem. Rev. (Washington, D.C.) **107**, 4797 (2007).

[18] S. A. Maier, *Plasmonics: Fundamentals and Applications* (Springer, Berlin, 2007).

[19] I. Romero, J. Aizpurua, G. W. Bryant, and F. J. García de Abajo, Opt. Express **14**, 9988 (2006).

[20] J. Mauritsson, P. Johnsson, E. Gustafsson, M. Swoboda, T. Ruchon, A. L'Huillier, and K. J. Schafer, Phys. Rev. Lett. **100**, 073003 (2008).

[21] See www.omicron.de for details of the Focus IS-PEEM instrument manufactured by Omicron Nanotechnology GmbH.

[22] L. Samuelson, Mater. Today **6**, 22 (2003).

[23] E. Hilner, U. Håkanson, L. E. Fröberg, M. Karlsson, P. Kratzer, E. Lundgren, L. Samuelson, and A. Mikkelsen, Nano Lett. **8**, 3978 (2008).

[24] A. Pietzsch, A. Föhlisch, M. Beye, M. Deppe, F. Hennies, M. Nagasono, E. Suljoti, W. Wurth, C. Gahl, K. Döbrich, and A. Melnikov, New J. Phys. **10**, 033004 (2008).

[25] J. J. Yeh and I. Lindau, At. Data Nucl. Data Tables **32**, 1 (1985).

[26] C. J. Powell and A. Jablonski, NIST Electron Effective-Attenuation-Length Database—Version 1.1, National Institute of Standards and Technology, Gaithersburg, MD, 2003.

[27] S. Collin, M. Merano, M. Gatri, S. Sonderegger, P. Renucci, J.-D. Ganière, and B. Deveaud, J. Appl. Phys. **98**, 094910 (2005).

[28] W. Knauer, J. Vac. Sci. Technol. **16**, 1676 (1979).

[29] B. W. Reed, J. Appl. Phys. **100**, 034916 (2006).

[30] S. Passlack, S. Mathias, O. Andreyev, D. Mittnacht, M. Aeschlimann, and M. Bauer, J. Appl. Phys. **100**, 024912 (2006).

[31] S. Hellmann, K. Rossnagel, M. Marczynski-Bühlow, and L. Kipp, Phys. Rev. B **79**, 035402 (2009).

[32] N. M. Buckanie, J. Göhre, P. Zhou, D. von der Linde, M. Horn-von Hoegen, and F.-J. Meyer zu Heringdorf, J. Phys.: Condens. Matter **21**, 314003 (2009).

[33] E. Bauer, Surf. Rev. Lett. **5**, 1275 (1998).

[34] See www.elmitec.de for details of the SPELEEM III instrument manufactured by Elmitec GmbH.

[35] A. Gloskovskii, D. A. Valdaitsev, M. Cinchetti, S. A. Nepijko, J. Lange, M. Aeschlimann, M. Bauer, M. Klimenkov, L. V. Viduta, P. M. Tomchuk, and G. Schönhense, Phys. Rev. B **77**, 195427 (2008).

[36] S. A. Maier and H. A. Atwater, J. Appl. Phys. **98**, 011101 (2005).

[37] B. Gilbert, R. Andres, P. Perfetti, G. Margaritondo, G. Rempfer, and G. De Stasio, Ultramicroscopy **83**, 129 (2000).

[38] G. F. Rempfer and O. H. Griffith, Ultramicroscopy **47**, 35 (1992).

[39] F. Lindner, W. Stremme, M. G. Schätzel, F. Grasbon, G. G. Paulus, H. Walther, R. Hartmann, and L. Strüder, Phys. Rev. A **68**, 013814 (2003).

[40] J. Boullet, Y. Zaouter, J. Limpert, S. Petit, Y. Mairesse, B. Fabre, and J. Higuet, Opt. Lett. **34**, 1489 (2009).

[41] S. Kim, J. Jin, Y.-J. Kim, I.-Y. Park, Y. Kim, and S.-W. Kim, Nature (London) **453**, 757 (2008).